

Energy harvesting with piezoelectric poly(γ -benzyl-L-glutamate) fibers prepared through cylindrical near-field electrospinning

 Cite this: *RSC Adv.*, 2014, 4, 21563

 Cheng-Tang Pan,^a Chung-Kun Yen,^a Liwei Lin,^b Yi-Syuan Lu,^c Hui-Wen Li,^a Jacob Chih-Ching Huang^c and Shiao-Wei Kuo^{*c}

In this study, we examined the electrical energy conversion and mechanical characteristics of piezoelectric fibers of the synthetic polypeptide poly(γ -benzyl-L-glutamate) (PBLG), prepared through cylindrical near-field electrospinning (CNFES) of a uniform macromolecular solution of PBLG in CH_2Cl_2 . A high electric field (from 5×10^6 to 1.5×10^7 V m^{-1}) provided the electrostatic force to pull the polymer solution into a Taylor cone, from which the PBLG fibers were electrospun, yielding piezoelectric PBLG fibers highly oriented in an α -helical conformation, as determined through Fourier transform infrared spectroscopic analysis. The orientation of the α -helical conformation of these polypeptide fibers was greater than those of other polymer piezoelectric materials; indeed, micro-tensile testing revealed that the Young's modulus and tensile stress of the fibers were 3.64 GPa and 60.54 MPa, respectively, greater than those of the typical piezoelectric polymer poly(vinylidene difluoride). The voltage outputs of single piezoelectric fibers reached as high as 89.14 mV with 8 M Ω resistance, with a maximum power output of 138.42 pW. PBLG piezoelectric fibers directly patterned on a cicada wing, with an interdigitated electrode for energy harvesting and a vibrational frequency of approximately 10–30 Hz, produced voltages ranging from 7.64 to 14.25 mV; such systems have potential applications as sensors and harvesters.

 Received 19th February 2014
 Accepted 1st May 2014

DOI: 10.1039/c4ra01452a

www.rsc.org/advances

Introduction

Electromechanical systems technology has recently been applied to miniaturize energy-harvesting and sensing devices; for example, functional piezoelectric materials are attracting increasing attention in various research fields, such as their development into flexible structures.^{1–3} Electrospinning is often used to fabricate piezoelectric fibers. In a typical far-field electrospinning process, fibers are emitted from a Taylor cone when a solution is subjected to a high-voltage electrostatic field.⁴ Highly aligned fibers are difficult to obtain through this method because the electrostatic force that stretches the fibers also bends them into complex shapes and causes chaotic whipping of the fiber jet, such that orderly fibers cannot be collected. Therefore, a direct-write electrospinning technique, using near-field electrospinning (NFES), has been developed to achieve controllable fiber deposition of various materials.^{5–8} Unlike conventional electrospinning, NFES requires only a small

electric voltage to produce continuous fibers having fine diameters; it is a cost-effective means of fabricating polymeric fibers.

Previous studies of piezoelectric polymer materials have generally used poly(vinylidene difluoride) (PVDF) as the substrate. For example, Andrew and Clark reported elevated levels of the β -crystalline phase (all-*trans* conformation) in electrospun PVDF fibers, due to both the stretching of the polymer chains and the electric field between the needle tip and the collector.⁹ In contrast, PVDF possesses a random coil conformation in solution, from which it requires higher energy to be poled by the electric field. As a result, the use of rod-like polymers is quite important when preparing new piezoelectric polymeric materials. For example, Farrar *et al.* prepared electrospun fibers of the polypeptide poly(γ -benzyl-L-glutamate) (PBLG) and measured a d_{33} piezoelectric coefficient of 25 pC N^{-1} ; this value did not deteriorate even after thermal treatment at 100 °C for over 24 h.¹⁰ Ren *et al.* combined electrospinning with a hot press method to prepare poled PBLG films exhibiting piezoelectricity in all of its d_{33} , d_{31} , and d_{14} modes; they found that these PBLG films possessed the matrix structure of the $C_{\infty v}$ group, the same as that of poled PVDF films.^{11,12} PBLG is a synthetic polypeptide that forms hierarchically ordered structures containing α -helices, which can be regarded as rigid rods stabilized by intramolecular hydrogen bonding interaction, and β -sheet secondary structures, stabilized by intermolecular

^aDepartment of Mechanical and Electro-Mechanical Engineering, National Sun Yat-Sen University, Kaohsiung 80424, Taiwan

^bDepartment of Mechanical Engineering and Berkeley Sensor and Actuator Center, University of California, Berkeley, California 94720, USA

^cDepartment of Materials and Optoelectronic Science, Center for Functional Polymers and Supramolecular Materials, National Sun Yat-Sen University, Kaohsiung 80424, Taiwan. E-mail: kuosw@faculty.nsysu.edu.tw

interactions, as fundamental secondary motifs.^{13,14} The α -helical structure of PBLG serves as a rigid-rod-like structure in the solid state and in solution.¹⁵ Although the dipole density of PVDF is higher than that of PBLG, PVDF features a random coil conformation in solution, resulting in a need for higher energy for poling by an electric field relative to that required for PBLG.^{16,17} In addition, the dipole direction for these polymers in a crystalline lattice is perpendicular to the polymer main chain direction. The electrospinning process produces a shear force and electric field in the same direction, thereby favoring a parallel arrangement of the polymer chains and the dipoles.

Our main goal for this study was to investigate the piezoelectric characteristics of PBLG, prepared using cylindrical near-field electrospinning (CNFES), for power generation. Using this approach, we could decrease the size of the piezoelectric PBLG fibers to the micro- and nanometer levels. These piezoelectric PBLG fibers possessed high flexibility, high toughness, and good thermal stability, suggesting that they could be applied for use in sensors and energy harvesters.

Experimental

CNFES process

During the CNFES processing of PBLG, alcohol with dehydration reaction was used to form BLG (γ -benzyl-L-glutamate). Triphosgene cyclization followed by addition of *n*-butylamine as a ring-opening polymeric initiator resulted in the formation of a PBLG powder having an α -helical structure, due to its high degree of polymerization.¹² The powder of PBLG [number-average molecular weight (M_n): 48 800 g mol⁻¹] was dispersed uniformly in CH₂Cl₂ through magnetic stirring for 30 min. The resulting PBLG solution was placed into a syringe. The experimental setup for CNFES processing is displayed in Fig. 1. The syringe was used as a container to fill up the solution. The contents were then injected using a precise infusion pump.

PBLG fibers were pulled out continuously and uniformly under a high electric field. A computer was used to control the signal conversion. The moving distance and speed of the XY-axis digital platform were controlled using computer software. A high-voltage power supply provided a maximum voltage of 40 kV. During the CNFES process, the syringes containing the PBLG solution were connected to a metal needle with copper wire to contact the high-voltage power supply. Under the high-voltage electric field, the prominently conical drops in the needle gradually became the Taylor cone.

Taguchi method

The Taguchi method was applied to decrease the experimental time. From signal-to-noise (*S/N*) analyses and analysis of variance (ANOVA), the optimal combination of processing parameters was determined. Experiments were then performed to verify these optimal processing parameters. The objective was to obtain high-output voltage in the piezoelectric fibers; thus, the quality characteristic was "the larger, the better". The related factors and levels are listed in Table 1.

Measurement of piezoelectric properties

The energy-harvesting device, displayed schematically in Fig. 2(a), was prepared over an area of 25 × 20 mm² on a flexible poly(ethylene terephthalate) (PET) substrate and packaged with aluminum conductive tape to form a structure. The purpose of using interdigital electrodes is to increase the current output. Before the *in situ* re-poling process, the piezoelectric polarization inside the polymer is aligned in one direction in which the polymers are spun across the interdigital electrodes. After the *in situ* re-poling process, the piezoelectric polarization inside the polymer is aligned permanently in an alternating direction, as shown in Fig. 2(b). The re-poling process can enhance the current output. The energy-harvesting device was characterized under periodic external strain provided by a tapping device

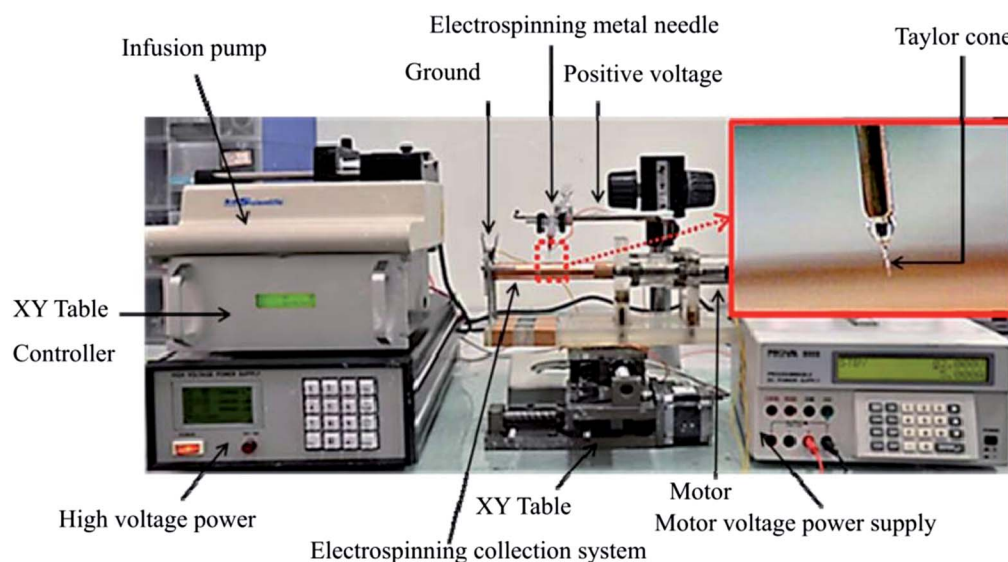


Fig. 1 Experimental set-up for the CNFES process.

Table 1 Levels and factors of Taguchi method with different experimental parameters to fabricate fibers

Factor	Level 1	Level 2	Level 3
(A) Concentration	16 wt%	18 wt%	20 wt%
(B) Electric field	$5 \times 10^6 \text{ V m}^{-1}$	10^7 V m^{-1}	$1.5 \times 10^7 \text{ V m}^{-1}$
(C) Rotating tangential speed	2094.4 mm s^{-1}	2618.0 mm s^{-1}	3141.6 mm s^{-1}
(D) Pump rate	1 mL h^{-1}	2 mL h^{-1}	3 mL h^{-1}
(E) Needle size	0.15 mm	0.2 mm	0.25 mm

operated at various frequencies; the PET substrate was tapped by the blade of this device. A schematic representation of the tapping measurement system is presented in Fig. 2(c). The energy-harvesting device was fixed at one end; the blade of the tapping device struck the energy-harvester at the other. In addition, a shaker was used to provide vibrating movement for the insect wing test, as displayed in Fig. 2(d). An NI9234 apparatus (maximum sampling frequency per channel: 51.2 kS/s; 24 bit resolution; 102 dB) was applied to measure the voltage. The current was measured using a CHI 611D instrument at an accuracy of 10^{-12} A ; the sampling rate was 0.005 s^{-1} .

Results and discussion

PBLG using CNFES

In the CNFES process, we used a rotating cylindrical glass tube (diameter: 20 mm; thickness: 1 mm; length: 200 mm) to collect the electrospun fibers. We placed copper foil onto the internal wall surface of this tube collector and attached an electric brush

for grounding purposes. Use of such a glass tube collector increased the break-down voltage significantly. By employing a DC motor to turn the tube collector, and controlling the uniaxial movement using an X-Y platform, we could collect the electrospun PBLG fibers in an orderly and continuous manner. When the electric field overcame the surface tension of the solution, the PBLG fibers were electrospun from the Taylor cone tip, which underwent electric poling, *in situ* mechanical stretching, and evaporation prior to orderly deposition of the fiber arrays. Fig. 3 displays a photograph of the bulk as-spun PBLG piezoelectric fibers as well as a scanning electron microscopy (SEM) image of individual fibers.

To investigate the effect of the solution concentration (varied from 10 to 18 wt%) on the PBLG fiber diameters, we fixed several of the experimental parameters: the molecular weight, the motion velocity of the X-Y stage (2 mm s^{-1}), the flow rate of the precision infusion pump (2 mL h^{-1}), and the inner diameter of the needle (0.2 mm). Upon varying the solution concentration from 10 to 18 wt%, the diameters of the piezoelectric fibers decreased from 43.85 to 17.25 μm [Fig. 4(a)]; we suspect that a higher concentration resulted in a smaller diameter because greater viscosity caused the fibers to agglomerate more readily. When we varied only the electric field from 2×10^6 to $1 \times 10^7 \text{ V m}^{-1}$, the diameters of the piezoelectric fibers decreased in a linear relationship from 46.8 to 7.5 μm ; thus, a higher electric field resulted in smaller fiber diameters [Fig. 4(b)]. Unlike the situation when using conventional far-field electrospinning, the effect of unstable stretching of fibers during the whipping process can be improved through the application of the stable tangential force during CNFES. Notably, insufficient voltages provided poor polarization, whereas excessive voltages led to

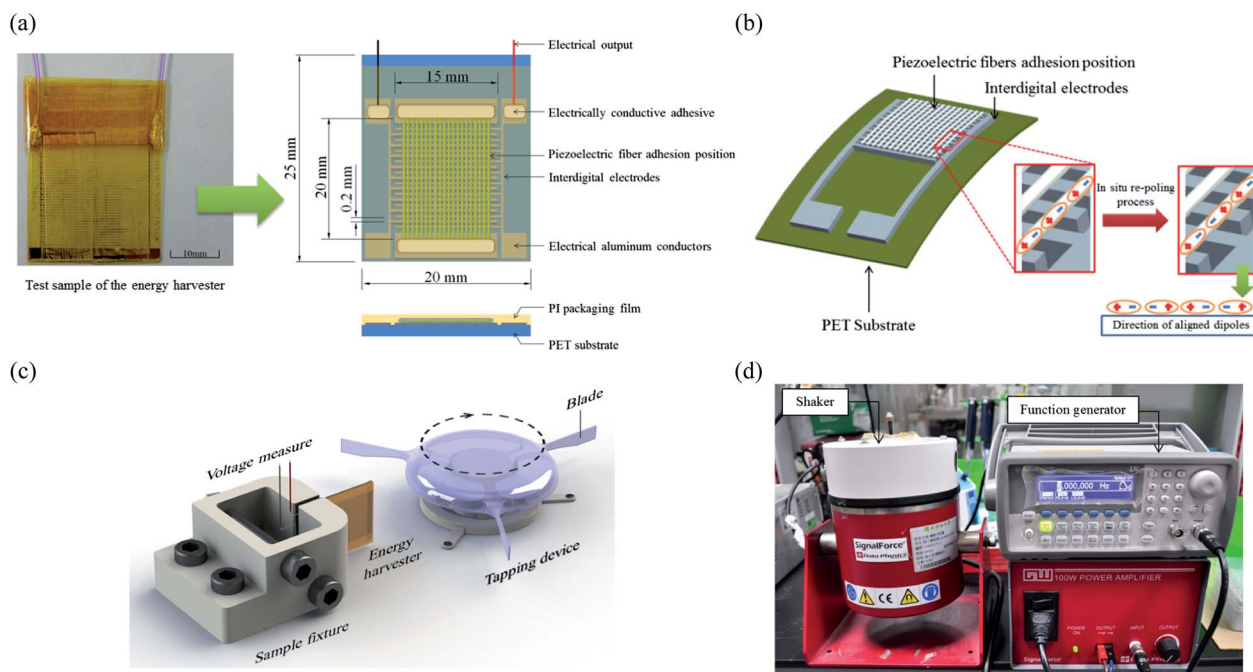


Fig. 2 (a) Schematic representation and test sample of the energy harvester. (b) A schematic diagram of fibers with *in situ* re-poling process. (c) Equipment used to measure the performance of energy harvester. (d) Shaker system for energy harvesting with an insect wing.

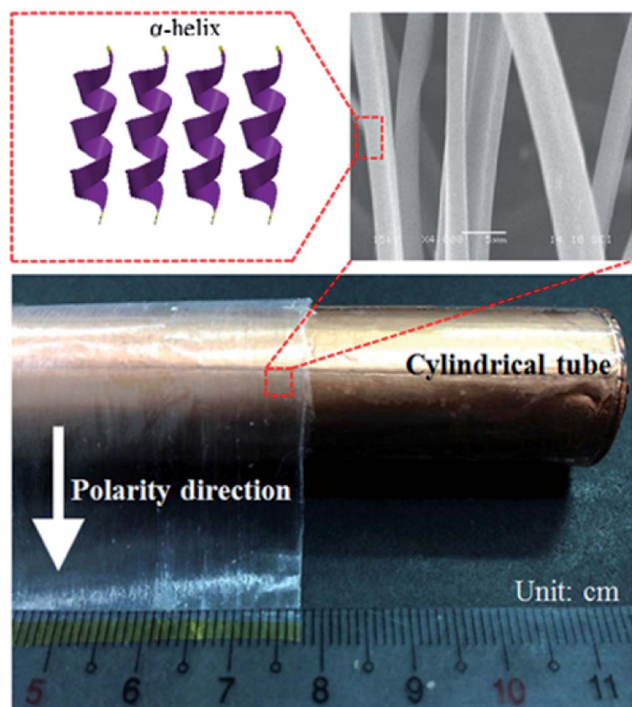


Fig. 3 Photograph and SEM image of PBLG piezoelectric fibers.

short circuiting, resulting in discontinuities in the electrospinning process. A short needle-to-collector distance can minimize the effect of the Coulombic repulsion force in the

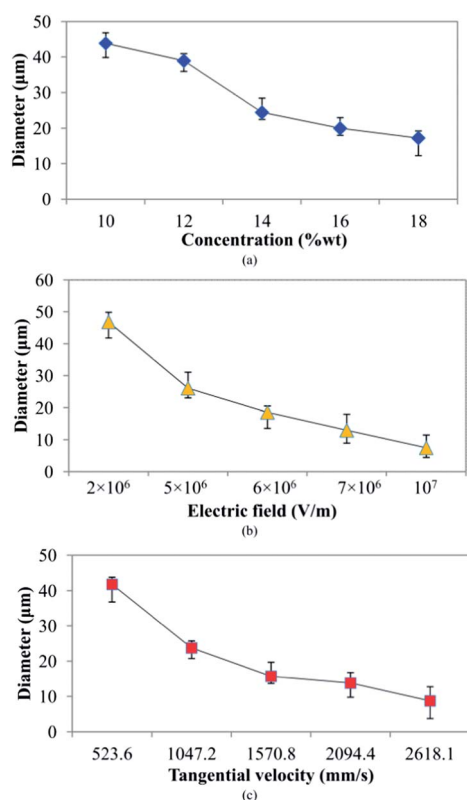


Fig. 4 Relationships between the fiber diameters and the (a) concentration, (b) electric field, and (c) tangential velocity.

polymer jet. In this case, insufficient space existed between the Taylor cone tip and the collector to whip and, thereby, stretch the fibers. When we varied only the rotating tangential velocity from 523 to 2618 mm s^{-1} , the diameter of the piezoelectric fibers decreased from 41.81 to 8.74 μm . When the tangential velocity of collection was slower than the speed of solution ejection, fibers bending was possible, thereby yielding fibers having rougher diameters. Therefore, the tangential velocity of the cylindrical tube affected the diameter of the piezoelectric fibers with an inverse relationship [Fig. 4(c)]. At an excessively low tangential velocity, the ejection rate of the fibers exceeded the collection rate, resulting in a disorderly collection. In contrast, excessively high tangential velocities caused the rate of collection of the fibers exceeded the ejection rate, resulting in broken fibers and a discontinuous collection. When the rotating tangential velocity of the tube collector was 524–2618 mm s^{-1} , the diameters of the PBLG fibers were less than 45 μm without discontinuities.

Taguchi method analysis

We used the Taguchi method to determine the optimal processing parameters of the PBLG piezoelectric fibers. Our goal was to produce energy harvesters displaying high power output. At a frequency of 18 Hz, we used the tapper to provide voltage signals in 18 different groups. From the Taguchi results, the optimal parameters (Fig. 5) were (A) a concentration of 18 wt%, (B) an electric field of $1.5 \times 10^7 \text{ V m}^{-1}$, (C) a tube tangential velocity of 2618 mm s^{-1} , (D) a syringe pump speed of 1 mL h^{-1} , (E) a needle size of 0.2 mm. In ANOVA studies, the contribution rates of the concentration, electric field, tube tangential velocity, syringe pump speed, and needle size were 0.50, 38.80, 17.20, 30.75, and 12.75%, respectively. Table 2 presents the relationships among these parameters. Under conditions applying the optimized parameters, the optimal voltage output was 77.15 mV; the minimum voltage was, however, 26.29 mV. Our results revealed that the electric field affected the voltage output and the power generation to the greatest degree. When the concentration was too dilute, the electrospinning conditions were unstable. On the other hand, the tangential velocity affected the diameters of the fibers as well as their continuity and uniformity. In addition, the needle size was also an important factor affecting the fiber diameters.

Characterization of PBLG fibers

PBLG is a synthetic polypeptide in which intramolecular hydrogen bonds stabilize an α -helical structure; these hydrogen bonds are aligned parallel to the central axis of the helical structure. Under a permanent dipole force, the amino acid residues can produce dipoles of high electric density, transforming the fibers into a state of permanent polarity exhibiting piezoelectric characteristics.⁹ Fig. 6 displays infrared spectra of the PBLG piezoelectric fibers, revealing an intense signal for the α -helical structure near 1655 cm^{-1} . An increase in the electric field resulted in a narrower absorption signal relative to that of the powder sample, due to the improved orientation enhancing the PBLG piezoelectric characteristics of the α -helical structure.

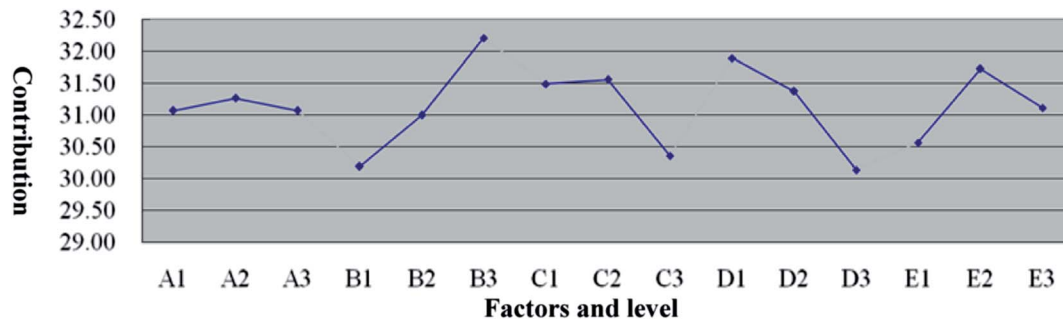


Fig. 5 Response graphs. (A–E are factors, and the 1–3 numbers are levels.)

Table 2 ANOVA of Taguchi method of PBLG piezoelectric fibers

	Changes of controlled factor (S)	Define of factor (DOF)	Variation (V)	Contribution rate (%)
(A) Concentration	0.152	2	0.076	0.50
(B) Electric field	12.335	2	6.167	38.80
(C) Tube tangential velocity	5.471	2	2.735	17.20
(D) Syringe pump speed	9.777	2	4.888	30.75
(E) Needle size	4.055	2	2.027	12.75
Total	31.790	10	15.893	100

We used an MTS tytron 250 micro-tensile testing machine to measure the mechanical properties of the PBLG piezoelectric fibers; we set the width of the piezoelectric fibers at 1 mm, the length at 15 mm, and the tensile rate at 0.015 mm s^{-1} , and used load cells to control the tensile force. Fig. 7(a) displays the tensile stretching process; Fig. 7(b) presents the stress/strain diagram plotted in terms of axial force and displacement. For PBLG, the maximum ultimate tensile stress was 60.54 MPa and Young's modulus was 3.64 GPa; for PVDF, these values were 37.85 MPa and 0.787 GPa, respectively.¹⁸ Thus, the mechanical properties of the PBLG samples prepared in this study were better than those of PVDF.

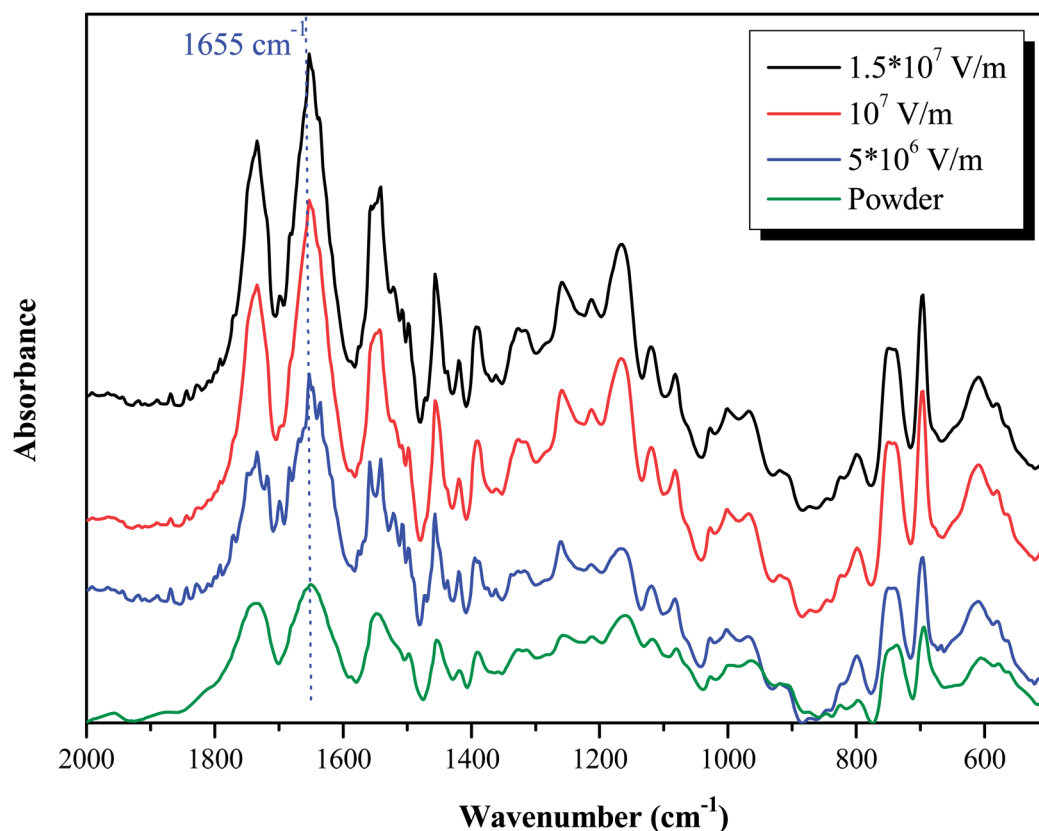


Fig. 6 FTIR spectra of powdered PBLG and PBLG piezoelectric fibers under various electric fields.

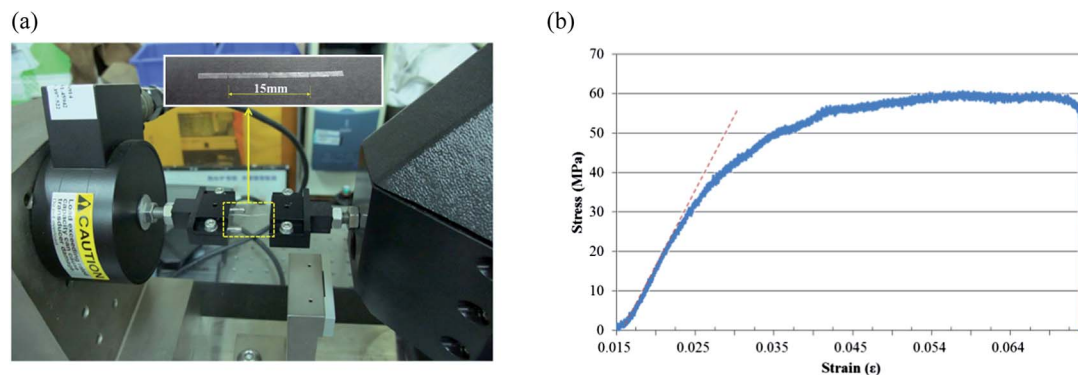


Fig. 7 (a) Device used to test the tensile properties of PBLG piezoelectric fibers. (b) Corresponding stress/strain curve.

Electrical probing of PBLG energy capture device

PBLG piezoelectric fibers generate power based on a Thévenin equivalents circuit [Fig. 8(a)], where the Thévenin impedance (Z_t) was designed to be equal to the external load (Z_{load}). Energy was produced by the sample interacting with the tapping device. We measured the voltages obtained in the presence of external loads of various resistances (0.01–16 M Ω). The maximum power output occurred for an external load resistor of 8 M Ω , because the internal resistance of the single-fiber PBLG energy harvesters was 8 M Ω . Fig. 8(b) reveals that the maximum voltage output was 33.27 mV; the corresponding power output was 138.42 pW. The output power of size dependence is strongly dependent on fiber counts, area and volume. In this study, the area of this piezoelectric device is 20 mm \times 15 mm in area, about 3000 pieces. When the density of the fibers inside the area is higher, the output power can be higher too. During the tapping test process, the piezoelectric bound charges induced a built-in potential in the energy harvester. The measurement result of open circuit voltage is shown in Fig. 9, which reveals the responses of the energy harvesting device under various frequencies ranging from 2.5 to 31.5 Hz for the same applied external strain. It shows that a higher frequency can induce a higher open circuit voltage. When a high frequency was applied to tap the harvester, it means a higher strain rate can be

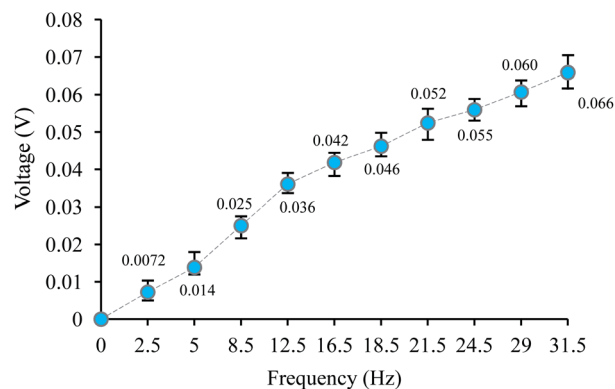


Fig. 9 Open circuit voltage as a function of frequency.

induced in the energy harvesting device. The output voltage during the tapping cycle increases with the frequency. Fig. 10 shows the measurement results at 18.5 Hz, the open circuit voltage of 0.045 V (see Fig. 10(a)), the short circuit current of 17.5 nA (Fig. 10(b)), the voltage of 0.031 V with an external load of 8 M Ω (Fig. 10(c)), and current of 4.19 nA with an external load of 8 M Ω (Fig. 10(d)).

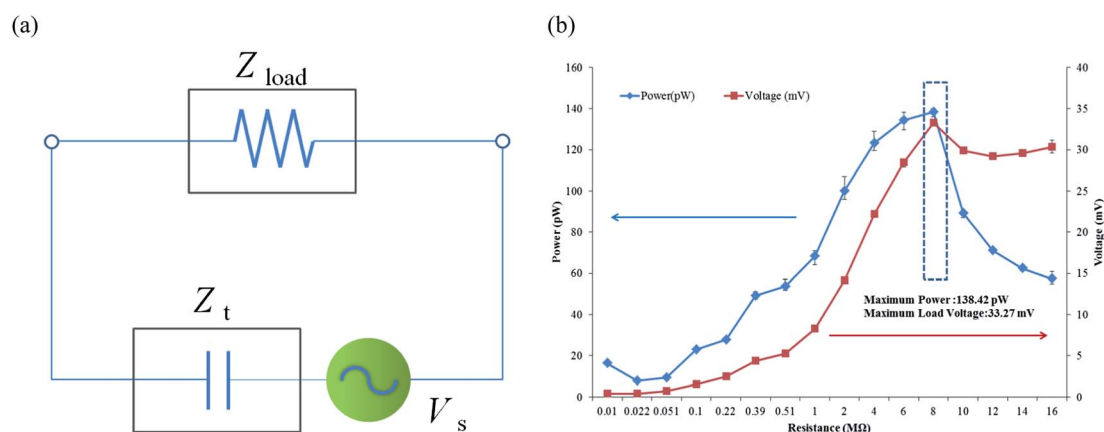


Fig. 8 (a) Thévenin equivalents circuit. (b) Load voltage and load power plotted with respect to load resistance of PBLG piezoelectric fibers.

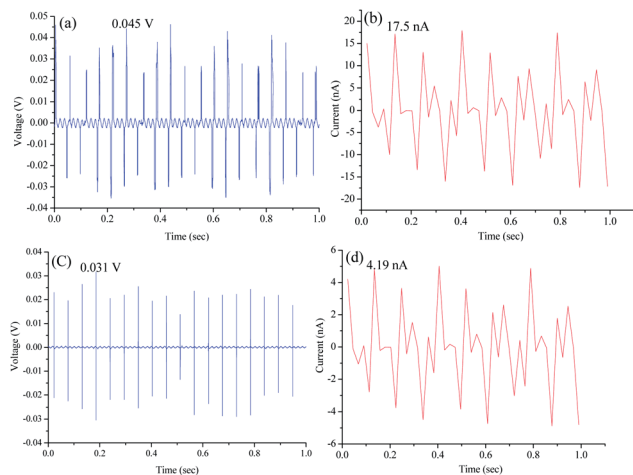


Fig. 10 Measurement result at 18.5 Hz (a) open circuit voltage (b) short circuit current (c) voltage with an external load of $8\text{ M}\Omega$ (d) current with an external load of $8\text{ M}\Omega$.

Piezoelectric properties measured using organism bionics

To test the applicability of our PBLG piezoelectric fibers, we fabricated them on cicada wings as energy-harvesting collectors, with interdigitated electrodes and conductive silver paste with a gap of 0.5 mm and a width of 5 mm. Fig. 11(a) displays the electrode that was electrospun with the PBLG fibers; Fig. 11(b) presents a photograph of the cicada wing placed on a shaker to simulate its flight.

Fig. 12 reveals that the voltage signal increased upon increasing the frequency. For example, we obtained voltage signals of 7.67, 10.42, and 14.25 mV and current signals of 16.78, 18.40, and 19.00 nA at frequencies of 10, 20, and 30 Hz, respectively. According to the piezoelectric theory $I = d_{33} EA\epsilon/\Delta t$, where I is the generated current, d_{33} is the piezoelectric charge constant, E is the Young's modulus, A is the cross-sectional area, and ϵ is the applied strain.¹⁹ Therefore, the electrical outputs of voltage and current increase with the strain rate. The reason of low frequency having more sub-peaks, that is because the substrate is still in the vibration. Some sub-peaks could be induced. The vibration test results in a mechanical strain distributed along the PBLG fibers. The strains of 0.04–0.1% at 10–30 Hz were measured, where a maximum peak voltage and current of 14.25 mV and 19 nA at 30 Hz were obtained, respectively.

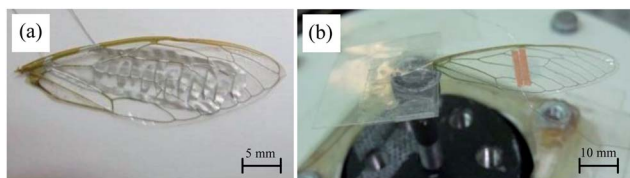


Fig. 11 Photographs of energy harvesting devices prepared on cicada wings. (a) Cicada wing functionalized with PBLG piezoelectric fibers. (b) Device positioned on a shaker.

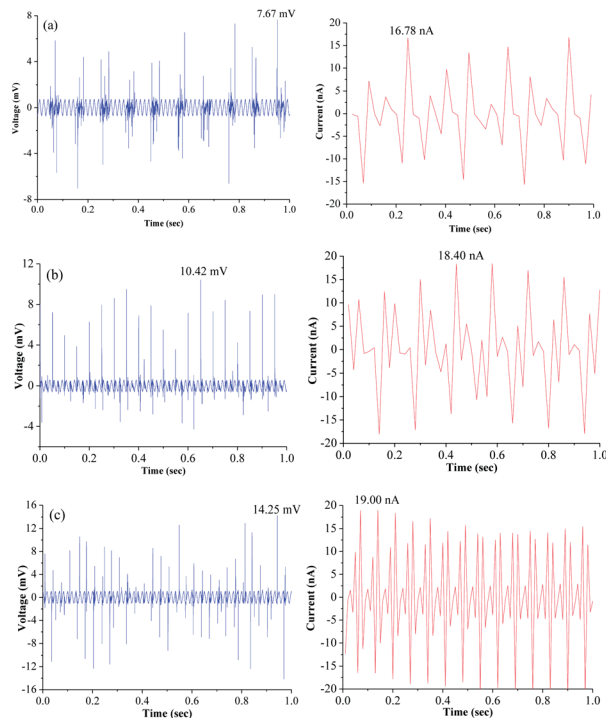


Fig. 12 Voltage and current measurements of a cicada wing energy-harvesting device functionalized with PBLG piezoelectric fibers and operated at (a) 10, (b) 20, and (c) 30 Hz.

Conclusions

We have used CNFES to fabricate PBLG piezoelectric fibers exhibiting permanent piezoelectricity. Relative to conventional far-field electrospinning, unstable stretching of the fibers during the whipping process can be improved through CNFES processing. An increase in the electric field led to significant enhancement in the piezoelectric characteristics as a result of the improved orientation of the α -helical structures. From tests of mechanical properties, we found that the mechanical stiffness of the PBLG piezoelectric fibers was greater than that of the PVDF piezoelectric fibers. Using the Taguchi method, we obtained the optimal process parameters to fabricate PBLG piezoelectric fibers. The electric field was the parameter that most affected the voltage output and power generation. When the concentration was too dilute, the electrospinning conditions were unstable. The tangential velocity affected the diameter of the fibers as well as their continuity and uniformity. The needle size also played an important role affecting the fiber diameters. We applied these PBLG fibers onto insect wings to generate voltage signals; such systems have potential for application as sensing devices and energy harvesters.

Acknowledgements

We thank the National Science Council of Taiwan for financial support under grant NSC-100-2628-E-110-006-MY3 and NSC-100-2221-E-110-029-MY3.

References

- 1 J. F. Nye, *Physical properties of crystals*, Clarend Press, Oxford, UK, 1957.
- 2 Z. Lin Wang and W. Wu, Nanotechnology-enabled energy harvesting for self-powered micro-/nanosystems, *Angew. Chem., Int. Ed.*, 2012, **51**, 11700–11721.
- 3 R. B. Williams and D. J. Inman, An overview of composite actuators with piezoceramic fibers, 2002 IMAC Conference (Conference & Exposition on Structural Dynamics), 2002, pp. 421–427.
- 4 (a) A. Theron, E. Zussman and A. L. Yarin, Electrostatic field-assisted alignment of electrospun nanofibers, *Nanotechnology*, 2001, **12**, 384–390; (b) G. Wang, Q. Dong, Z. Ling, C. Pan, C. Chang and J. S. Qiu, Hierarchical activated carbon nanofiber webs with tuned structure fabricated by electrospinning for capacitive deionization, *J. Mater. Chem.*, 2012, **41**, 21819–21823.
- 5 D. H. Reneker, A. L. Yarin, H. Fong and S. Koombhongse, Bending instability of electrically charged liquid jets of polymer solutions in electrospinning, *J. Appl. Phys.*, 2000, **87**, 4531–4547.
- 6 D. Sun, C. Chang, S. Li and L. W. Lin, Near-field electrospinning, *Nano Lett.*, 2006, **6**, 839–842.
- 7 Y. K. Fuh, L. C. Lien and S. Y. Chen, High-throughput production of nanofibrous mats via a porous materials electrospinning process, *J. Macromol. Sci., Part B: Phys.*, 2012, **51**, 1742–1749.
- 8 C. Chang, K. Limkrailassiri and L. W. Lin, Continuous near-field electrospinning for large area deposition of orderly nanofiber patterns, *Appl. Phys. Lett.*, 2008, **93**, 123111.
- 9 J. S. Andrew and D. R. Clarke, Effect of electrospinning on the ferroelectric phase content of polyvinylidene difluoride fibers, *Langmuir*, 2008, **24**, 670–672.
- 10 D. Farrar, K. Ren, D. Cheng, S. Kim, W. Moon, W. L. Wilson, J. E. West and S. M. Yu, Permanent polarity and piezoelectricity of electrospun α -helical poly(α -amino acid) fibers, *Adv. Mater.*, 2011, **23**, 3954–3958.
- 11 K. Ren, W. L. Wilson, J. E. West, Q. M. Zhang and S. M. Yu, Piezoelectric property of hot pressed electrospun poly(γ -benzyl- α -L-glutamate) fibers, *Appl. Phys. A*, 2012, **107**, 639–646.
- 12 Z. H. Liu, C. T. Pan, L. W. Lin, J. C. Huang and Z. Y. Ou, Direct-write PVDF nonwoven fiber fabric energy harvesters via the hollow cylindrical near-field electrospinning process, *Smart Mater. Struct.*, 2014, **23**, 025003–025014.
- 13 S. W. Kuo, H. F. Lee, W. J. Huang, K. U. Jeong and F. C. Chang, Solid state and solution self-assembly of helical polypeptides tethered to polyhedral oligomeric silsesquioxanes, *Macromolecules*, 2009, **42**, 1619–1626.
- 14 P. C. Li, Y. C. Lin, M. Chen and S. W. Kuo, Self-Assembly Structures of PEGylation Polypeptide Block Copolymers Synthesized Using a Combination of ATRP, ROP, and Click Chemistry, *Soft Matter*, 2013, **9**, 11257–11269.
- 15 S. W. Kuo and C. J. Chen, Functional polystyrene derivatives influence the miscibility and helical peptide secondary structures of poly(benzyl-L-glutamate), *Macromolecules*, 2012, **45**, 2442–2452.
- 16 A. J. Lovinger, Ferroelectric polymers, *Science*, 1983, **220**, 1115–1121.
- 17 Y. Takase, J. W. Lee, J. I. Scheinbeim and B. A. Newman, High-temperature characteristics of nylon-11 and nylon-7 piezoelectrics, *Macromolecules*, 1991, **24**, 6644–6652.
- 18 Z. H. Liu, C. T. Pan, L. W. Lin, H. W. Li, Z. Y. Ou and J. C. Huang, “Mechanical properties of piezoelectric PVDF/MWCNT fibers prepared by flat/hollow cylindrical near-field electrospinning process”, The 8th Annual IEEE International Conference by Nano/Micro Engineered and Molecular Systems, 2013, pp. 707–710.
- 19 J. Sirohi and I. Chopra, Fundamental understanding of piezoelectric strain sensors, *J. Intell. Mater. Syst. Struct.*, 2000, **11**, 246–275.